


Article

Blocking *IbmiR319a* Impacts Plant Architecture and Reduces Drought Tolerance in Sweet Potato

Lei Ren ^{1,2,†}, Tingting Zhang ^{1,2,†}, Haixia Wu ^{1,2}, Xinyu Ge ^{1,2}, Huihui Wan ^{1,2}, Shengyong Chen ³, Zongyun Li ^{1,2} , Daifu Ma ^{4,*} and Aimin Wang ^{1,2,*}

¹ Institute of Integrative Plant Biology, School of Life Science, Jiangsu Normal University, Xuzhou 221116, China; r15905217129@163.com (L.R.); 15396884589@163.com (T.Z.); whx2734793896@163.com (H.W.); gxy20000703@163.com (X.G.); wanyang2003@outlook.com (H.W.); zongyunli@jsnu.edu.cn (Z.L.)

² Jiangsu Key Laboratory of Phylogenomics & Comparative Genomics, School of Life Science, Jiangsu Normal University, Xuzhou 221116, China

³ Zhanjiang Academy of Agricultural Sciences, Zhanjiang 524094, China; chengreen-1980@163.com

⁴ Key Laboratory for Biology and Genetic Breeding of Sweetpotato (Xuzhou), Ministry of Agriculture/Jiangsu Xuzhou Sweetpotato Research Center, Xuzhou Institute of Agricultural Sciences, Xuzhou 221131, China

* Correspondence: daifuma@163.com (D.M.); aiminwang@jsnu.edu.cn (A.W.); Tel.: +86-516-82189200 (D.M.); +86-516-83400033 (A.W.)

† These authors contributed equally to this work.

Abstract: MicroRNA319 (*miR319*) plays a key role in plant growth, development, and multiple resistance by repressing the expression of targeted *TEOSINTE BRANCHED/CYCLOIDEA/PCF (TCP)* genes. Two members, *IbmiR319a* and *IbmiR319c*, were discovered in the *miR319* gene family in sweet potato (*Ipomoea batatas* [L.] Lam). Here, we focused on the biological function and potential molecular mechanism of the response of *IbmiR319a* to drought stress in sweet potato. Blocking *IbmiR319a* in transgenic sweet potato (MIM319) resulted in a slim and tender phenotype and greater sensitivity to drought stress. Microscopic observations revealed that blocking *IbmiR319a* decreased the cell width and increased the stomatal distribution in the adaxial leaf epidermis, and also increased the intercellular space in the leaf and petiole. We also found that the lignin content was reduced, which led to increased brittleness in MIM319. Quantitative real-time PCR showed that the expression levels of key genes in the lignin biosynthesis pathway were much lower in the MIM319 lines than in the wild type. Ectopic expression of *IbmiR319a*-targeted genes *IbTCP11* and *IbTCP17* in *Arabidopsis* resulted in similar phenotypes to MIM319. We also showed that the expression of *IbTCP11* and *IbTCP17* was largely induced by drought stress. Transcriptome analysis indicated that cell growth-related pathways, such as plant hormonal signaling, were significantly downregulated with the blocking of *IbmiR319a*. Taken together, our findings suggest that *IbmiR319a* affects plant architecture by targeting *IbTCP11/17* to control the response to drought stress in sweet potato.

Keywords: sweet potato; microRNA319; TCP transcription factor; drought stress



Citation: Ren, L.; Zhang, T.; Wu, H.; Ge, X.; Wan, H.; Chen, S.; Li, Z.; Ma, D.; Wang, A. Blocking *IbmiR319a* Impacts Plant Architecture and Reduces Drought Tolerance in Sweet Potato. *Genes* **2022**, *13*, 404. <https://doi.org/10.3390/genes13030404>

Academic Editor: Qing Yang

Received: 16 January 2022

Accepted: 21 February 2022

Published: 24 February 2022

Publisher's Note: MDPI stays neutral with regard to jurisdictional claims in published maps and institutional affiliations.



Copyright: © 2022 by the authors. Licensee MDPI, Basel, Switzerland. This article is an open access article distributed under the terms and conditions of the Creative Commons Attribution (CC BY) license (<https://creativecommons.org/licenses/by/4.0/>).

1. Introduction

Drought is a major environmental factor causing abiotic stress [1–3]. Severe drought restricts crop growth and significantly reduces yield worldwide [4,5]. It is therefore essential that crops with drought tolerance traits are produced. Generally, the responses of plants to abiotic stress are similar, especially in the first phase—a rapid osmotic phase that inhibits shoot growth [6]. At the physiological level, the symptoms of drought damage include wilting, growth retardation through reduced photosynthetic capacity (especially the lost function of PSII) [7], discoloration, abnormal ripening, and so on [8].

Although sweet potato (*I. batatas*) is a drought-tolerant root crop, dry matter accumulation and root tuber enlargement are inhibited under drought stress, which seriously

hampers production [9]. Genetic engineering methods can be used to improve drought tolerance. At the molecular level, the ectopic expression of enzyme genes, such as *XvSap1* (*Xerophyta viscosa* stress-associated proteins) [10], *SoBADH* (spinach betaine aldehyde dehydrogenase) [11], *AgcodA* (*Arthrobacter globiformis* choline oxidase), *AtHDG11* (*Arabidopsis thaliana* Homeodomain glabrous 11) [12], and *XvAld1* (*Xerophyta viscosa* Aldose reductase 1) [13], improves drought tolerance in sweet potato. Overexpression of endogenous enzyme genes and structural genes, such as *IbC4H* (cinnamate 4-hydroxylase) [14], *IbMIPS1* (myo-inositol-1-phosphate synthase) [15], *IbCBF3* (dehydration-responsive element-binding/C-repeat-binding factor) [16], *IbNHX2* (Na^+/H^+ antiporters) [17], *IbBT4* (BTB-TAZ-domain protein) [18], and *IbARF5* (auxin response factor) [19], or transcription factors, such as *IbbZIP1* (basic region/leucine zipper motif transcription factor) [20], *IbABF4* (abscisic acid (ABA)-responsive element binding factors) [21], and *IbMYB116* [22], can also improve the drought tolerance of transgenic sweet potato plants.

The above studies mainly focused their attention on maneuvering downstream gene functioning in the physiological responses of osmotic or ionic adjustment in sweet potato. The upstream regulatory networks of stress responses in sweet potato are still largely unknown. Increasingly more research has revealed that microRNAs (miRNAs) are involved in various plant stress responses by regulating their target genes, which are mainly transcription factors, forming a complex regulatory network and playing key roles in the gene regulation networks [23]. MiRNAs are small single-stranded non-protein-coding RNAs usually 20–24 nucleotides (nt) in length [24,25] that regulate gene expression by mRNA cleavage at the post-transcriptional level or translational repression through base pairing with the complementary sequence within the target mRNAs involved in plant growth, development, and also various plant stress responses [26]. MicroRNA319 (miR319) belongs to one of the most ancient and conserved miRNA families [27]. Increasingly more studies have shown that miR319 targets transcription factor *TCP* genes, playing vital roles in plant morphogenesis and reproduction [28–30], and also responding to multiple biotic and abiotic stresses [31–34]. In leaf development, the overexpression of miR319 or suppression of its target *TCP* genes contributed to directly regulate the progression of the cell cycle genes *ICK1/KRP1* to control the G₂-M phase of the cell cycle [30], causing an uneven leaf shape and curvature and resulting in serrated leaves in *Arabidopsis* [28]. The miR319-*TCP* module also affects the balance between mitosis and endoreduplication [35]. In the response to various stresses, overexpressing *shamiR319d* enhanced temperature tolerance by inhibiting the expression of *GAMYB-like1* and further altering temperature and reactive oxygen species' [36] signal transduction in tomato [37]. The overexpression of both *OsaMIR319a* and *OsaMIR319b* led to enhanced cold tolerance by downregulating *OsPCF5* and *OsPCF8* in rice [31]. *PvmiR319*, targeting *PvPCF5*, promoted ethylene (ET) synthesis to improve salt tolerance in switchgrass (*Panicum virgatum* L.) [38]. The miR319a/*TCP* module participated in trichome initiation synergistically with gibberellic acid (GA) signaling and improved insect defenses in *Populus tomentosa* [34].

Although miR319-mediated changes in plant morphology and the response to biotic and abiotic stresses have been well studied in many plants, there is limited information available for sweet potato, which is a widely cultivated and important tuberous crop. In this study, we explored the function of the miR319-*TCP* module in the plant architecture and the tolerance of drought in sweet potato. We produced transgenic sweet potato plants with inhibited *IbmiR319a* by miRNA target MIMICS (MIM319), which has been proven to be efficient in inhibiting miRNA function [39]. Blocking *IbmiR319a* not only affected plant architecture, but also reduced drought tolerance in sweet potato seedlings. Moreover, *IbTCP11/17*, two target genes of *IbmiR319a*, participated in drought stress. Collectively, the results suggest that the miR319-*IbTCP* module modulates plant architecture, thereby influencing drought tolerance in sweet potato.

2. Materials and Methods

2.1. Plant Materials

The sweet potato cultivar 'Xushu 22' wild type (WT), developed by the Sweet Potato Research Institute of the China Agriculture Academy of Science (SPRI-CAAS), was used as a donor for genetic transformation. Untransformed and transgenic plants subcultured from in vitro plantlet cultures were transferred into plastic pots (18 cm in diameter) containing dark soil and vermiculite at a ratio of 2:1 (*v/v*) and grown in a growth chamber under a 16 h light/8 h dark photoperiod at 25 ± 3 °C. Shoots that were 3–4 cm in height were transplanted into the field in early May in 2020 for evaluation of the phenotype and agronomic traits at the Xuzhou experimental station (E 117°17.48', N 34°16.95') of the Sweet Potato Research Institute of the Chinese Academy of Agricultural Sciences (SPRI-CAAS).

The *Arabidopsis thaliana* plants were grown in an artificial climate chamber at 22 ± 3 °C and 16 h light/8 h dark photoperiod.

2.2. Plasmid and Sweet Potato Genetic Transformation

p35S-MIM319, the miR319 target mimicry vector, was constructed as previously described [39]. Genetic transformation of sweet potato was conducted according to the previously described method by Yang [40].

2.3. Vector Construction and Arabidopsis Transformation

The full-length CDSs of the *IbTCP11/17* sequences were amplified using gene-specific primers, and then cloned into the *SacI* and *KpnI* sites of the binary vector pCAMBIA1300 containing the cauliflower mosaic virus 35S promoter to create the overexpression vectors *IbTCP11OE* and *IbTCP17OE*, respectively, and then transferred into *Agrobacterium tumefaciens* strain LBA4404. *Arabidopsis* transformation was performed using the floral-dip method to produce transgenic *Arabidopsis* plants [41], which were subsequently grown in pots to produce T₃ seeds by screening with 50 mg/L hygromycin.

2.4. RNA Isolation and qRT-PCR Analysis

Total RNAs were extracted using TRIzol (Invitrogen, Carlsbad, CA, USA) and then treated with RNase-free DNase I (Sigma, St. Louis, MO, USA) to remove contaminated genomic DNA. The RNA integrity was determined by 1% gel electrophoresis, and the RNA concentration was measured using a NanoDrop spectrophotometer (ND1000, Technologies, Wilmington, NC, USA).

For quantitative real-time PCR (qRT-PCR) analyses of mRNA for the genes, 2 µg of RNA per sample were reverse-transcribed to produce cDNA using the HiScript II 1st Strand cDNA Synthesis Kit (Vazyme, Shanghai, China). The qRT-PCR was performed with the ClonExpress Ultra One Step Cloning Kit (Vazyme), and the *IbActin* gene was used as an internal control. Data from three biological samples were collected, and the mean values were normalized to *IbActin*.

For miRNA quantitative analysis, the stem-loop RT-PCR method was used. One microgram of DNase-treated RNA was converted into cDNA using the First Strand cDNA Synthesis Kit (Takara, Dalian, China). The miR319-specific primer and miRNA universal primer (URP) were used for qRT-PCR. *IbActin* RNA was used as an endogenous control. The abundance of *miR319* was normalized to *IbActin* RNA as a reference.

The relative abundance of gene expression was determined using the $2^{-\Delta\Delta Ct}$ method [42]. All gene expression data are from three biological replicates with three technical replicates for each biological sample. The sequences for the primers are listed in Supplementary Table S1.

2.5. Microscopic Observations

For paraffin sectioning, the first fully expanded fresh leaves or stems were fixed in 0.1 M sodium phosphate buffer containing 2.5% (*v/v*) glutaraldehyde for 24 h. Samples were dehydrated through an alcohol series, followed by resin-alcohol grading, and embed-

ding in acrylic resin. Semi-thin sections of 1 mm thickness were obtained using the standard rotary microtomy technique and stained with Safranin O-Fast Green. Photomicrographs were taken under 10× and 20× objectives of the fluorescence microscope (Axiolab, Zeiss, MC80 Dx Camera).

For epidermis cell observation, the first fully expanded fresh leaves were folded and torn gently from the fold, and a small piece of torn white film was made into a temporary slide and observed with a light microscope. The length and width of the epidermis cells were measured, and the stoma were counted.

2.6. Lignin Deposition Experiment and Lignin Content Measurement

Analysis of the Klason lignin content was performed with the sulfuric acid digestion method [43]. For lignin deposition staining with toluidine blue, hand-cut sections of the third internode were cut from two-month-old plants in the greenhouse. Free-hand slices were made and stained with toluidine blue (toluidine blue staining solution, Servicebio, Wuhan, China) for about 2 min, rinsed with water, and then observed under an optical microscope.

2.7. Measurement of Breaking Force

The third internodes from the top of two-month-old MIM319 and WT seedlings were used for measurements. The force required to break the stems was recorded with a texture analyzer (Shimadzu, EZ Test, Kyoto, Japan) with the detector TA52. Ten plants of each of MIM319 and WT were measured, and all measurements were taken under the same conditions.

2.8. Analysis of Drought Tolerance

The cuttings of MIM319 and WT were used for the drought stress experiments. The cuttings transplanted for 2 weeks were watered sufficiently for 1 week, following which water was withheld for 4 weeks to simulate drought stress. The physiological indexes, including malondialdehyde (MDA) and proline contents, and antioxidant enzyme system activity, were measured with assay kits (Nanjing Jiancheng Bioengineering Institute, Nanjing, China) as described before [14]. Each data point was the average of three replicates. Approximately 20 cuttings of each line were used for each experiment, and at least 3 replicates of each experiment were performed, and the results were consistent. The result from one set of experiments is presented herein.

2.9. Gene Expression Analysis

The first fully expanded leaves of MIM319 and WT plants subjected to drought stress for one week were used to analyze the relative expression level of the genes related to stress responses, including target genes *IbTCP11/17*, proline biosynthesis, and the ROS-scavenging system, using qRT-PCR. The sequences of the specific primers are listed in Supplementary Table S1.

2.10. Transcriptome Analysis

Total RNA was extracted from the shoots of MIM319 and WT grown in a transplanting box for 4 weeks using the TRIzol method (Invitrogen, Carlsbad, CA, USA), and 1 g of RNA was used for Illumina RNA-Seq. Transcriptome sequencing and de novo transcriptome assembly and evaluation were performed by Huada (Beijing, China). After filtering with SOAPnuke (v1.5.2). (Available online: <https://github.com/BGI-flexlab/SOAPnuke>, accessed on 5 August 2021), clean reads were obtained and stored in FASTQ format. The clean reads were mapped to the reference genome using HISAT2 (v2.0.4) (Available online: <http://www.ccb.jhu.edu/software/hisat/index.shtml>, accessed on 5 August 2021). Bowtie2 (v2.2.5) (Available online: <http://bowtiebio.sourceforge.net/%20Bowtie2%20/index.shtml>, accessed on 5 August 2021) was used to align the clean reads to the reference coding gene set, and then the expression level of the genes was calculated by

RSEM (v1.2.12) (Available online: <https://github.com/deweylab/RSEM>, accessed on 5 August 2021). A heatmap was produced using pheatmap (v1.0.8) (Available online: <https://cran.r-project.org/web/packages/pheatmap/index.html>, accessed on 5 August 2021) according to the gene expression in different samples. The differential expression analysis was performed using DESeq2 (v1.4.5) (Available online: <http://www.bioconductor.org/packages/release/bioc/html/DESeq2.html>, accessed on 5 August 2021) with Q-values ≤ 0.05 . Gene Ontology (GO; Available online: <http://www.geneontology.org/>, accessed on 5 August 2021) and Kyoto Encyclopedia of Genes and Genomes (KEGG; Available online: <https://www.kegg.jp/>, accessed on 5 August 2021) enrichment analyses of differentially expressed genes (DEGs) were performed by Phyper (Available online: https://en.wikipedia.org/wiki/Hypergeometric_distribution, accessed on 5 August 2021) based on the hypergeometric test. The significance levels of the terms and pathways were corrected by the Q-value with a rigorous threshold (Q value ≤ 0.05) by Bonferroni [44]. All the above website accessed on 5 November 2021.

2.11. Statistical Analysis

The Student's *t*-test was used to analyze all the data presented as the mean \pm SE. *p*-values of <0.01 , or <0.05 were considered to be statistically significant.

3. Results

3.1. Identification and Characterization of *IbmiR319* in Sweet Potato

MiR319 was the first miRNA identified through positive genetic screening [28]. In previous studies, we constructed an miRNA library of sweet potato based on high-throughput sequencing [2], and two members of the miR319 family (*IbmiR319a* and *IbmiR319c*) with different matured miRNA sequences were found (Figure 1A,B). Both *IbmiR319* precursors were supported by cDNAs in the public database (<http://public-genomes-ngs.molgen.mpg.de/SweetPotato/>, accessed on 5 August 2021). The gene encoding *IbmiR319a* was located in chromosome (chr) 15 from 1889,2867 to 1889,3043 (Supplement Figure S1A), while that of *IbmiR319c* was located in chr 2 from 4761,9325 to 4761,9514 (Supplement Figure S1B).

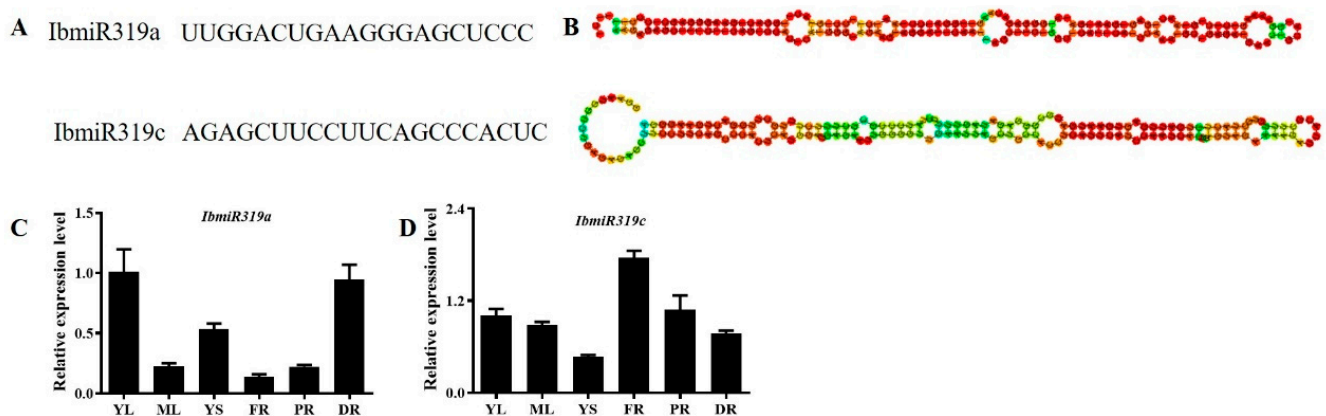


Figure 1. The microRNA319 family contains two members in sweet potato. (A): Sequence of mature *IbmiR319a* and *IbmiR319c*. (B): The secondary structure of the precursor sequence of *IbmiR319a* and *IbmiR319c*. (C,D): The expression patterns of *IbmiR319a* and *IbmiR319c*. YL: young leaf; ML: mature leaf; YS: young stem; FR: fibrous root; PR: pencil root; DR: developing root.

To determine the expression patterns of *IbmiR319*, we conducted stem-loop qRT-PCR of *IbmiR319* mature transcripts in the leaves, stems, fibrous roots, pencil roots, and storage roots (Figure 1C,D). *IbmiR319a* showed a higher expression level in the young organs or vigorously growing organs, especially the young leaf and developing root, while *IbmiR319c* showed a higher expression level in the fibrous roots, indicating that *IbmiR319a* may play an important role in development. We therefore focused our attention on the functional analysis of *IbmiR319a*.

3.2. Generation of Transgenic Sweet Potato Plants with *miR319a* Blocked

To investigate the function of *IbmiR319a* in sweet potato, we constructed a plasmid overexpressing *IbmiR319a* target mimicry (MIM319), intending to sequester the normal expression of native *IbmiR319a*, and transformed it into the sweet potato variety ‘Xu22’, which was used as WT. We obtained seven independent transgenic MIM319 plants, among which five positive plants named m3-2, m3-3, m3-8, m3-9, and m3-10 were verified (Supplement Figure S2A–D). To determine the expression level of *IbmiR319a*, these five positive transgenic lines were analyzed using stem-loop qRT-PCR, with WT as the control. The abundance of *IbmiR319a* mature transcripts in transgenic plants was lower than that in WT (Figure 2A), suggesting that the MIM319 fusion plasmids were successfully expressed in sweet potato, and normal *IbmiR319a* was successfully blocked. One independent transgenic line m3-9, with relatively lower *IbmiR319a* expression levels, was chosen as MIM319 for further analysis.

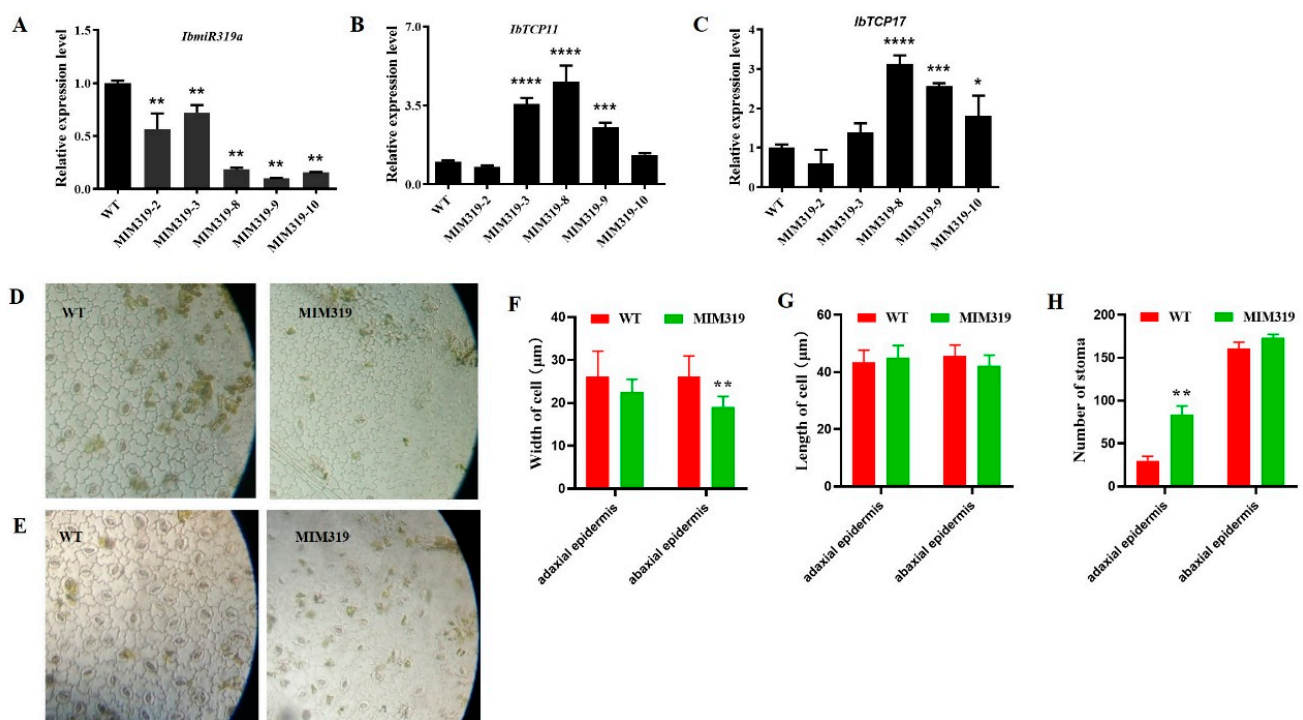


Figure 2. Gene expression level and light microscopic observation of MIM319 transgenic sweet potato plants. (A): Expression level of mature *IbmiR319a* in MIM319 transgenic sweet potato lines and WT. (B,C): Expression level of the target genes *IbTCP11/17* in MIM319 transgenic sweet potato lines and WT. (D): Images of leaf adaxial epidermal cells of the WT and MIM319 plants under the light microscope. (E): Images of leaf abaxial epidermal cells of the WT and MIM319 plants under the light microscope. (F): Quantitative measurement of the maximum leaf epidermis cell width of WT and MIM319 transgenic plants ($n = 100$). (G): Quantitative measurement of the maximum leaf epidermis cell length of WT and MIM319 lines ($n = 100$). (H): Statistical analysis of the total stomata number in WT and MIM319 transgenic plants ($n = 30$). Data are presented as means \pm SE, and error bars represent SE. *, **, ***, **** indicate significant differences between transgenic and control plants at $p < 0.05, 0.01, 0.001, 0.001$ by Student's t -test.

3.3. Expression Level of the Putative *IbmiR319a* Target Genes Was Upregulated in MIM319 Transgenic Sweet Potato

In general, miRNAs play important roles by post-transcriptionally regulating their target genes. In sweet potato, *IbmiR319a* was predicted to target Transcript comp94376_c4 and comp87184_c3 according to our degradation and transcriptome sequencing results [2]. Using these sequences as a reference in the BLAST search in the genomics database for

its 2 wild ancestors (*Ipomoea trifida* and *Ipomoea triloba*) (Available online: <http://sweetpotato.uga.edu/>, accessed on 5 August 2021), we found that they were 98% identical to sequence ID CP025644.1 on chr 1 and CP025653.1 on chr 10 of *I. trifida* (Supplement Figure S3A,B). We named them *IbTCP11* and *IbTCP17* according to their chromosome location [45]. This complementary area between the targets and *IbmiR319a* was shown in our previous study through the psRNA Target tool [45]. We further checked the predicted *IbTCP11* and *IbTCP17* transcript levels in MIM319 plants by qRT-PCR. The result showed that *IbTCP11/17* increased the mRNA levels in the leaves of transgenic MIM319 plants compared to the WT (Figure 2B,C). Considering that MIM319 plants showed a relatively low level of mature *IbmiR319a* expression in the leaves where the miR319-targeted *IbTCP11/17* had a high level of expression, we assumed that blocking *IbmiR319a* could promote the high mRNA levels of the targeted genes.

3.4. Blocking *IbmiR319a* in Sweet Potato Caused Pleiotropic Phenotype Changes

As previously reported, the highly conserved ancient miR319 plays an important role in plant development [31]. Moreover, overexpressing or blocking *miR319* resulted in pleiotropic phenotype changes. All positive MIM319 transgenic sweet potatoes blocking *IbmiR319a* showed similar phenotypes. Despite the narrow and small leaves previously reported [45], a more thorough investigation was conducted. Microscopic analysis of the leaf samples showed that the epidermal cells of MIM319 were shaped like irregular squares while the WT cells were irregular rectangles (Figure 2D,E). The average length of the adaxial and abaxial leaf epidermis cells was 45 and 42.22 μm in MIM319, respectively, which was not obviously different from that of the WT (43.33 and 45.56 μm , respectively). However, the average width of the abaxial and adaxial leaf epidermis cells was 19.11 and 22.56 μm in MIM319, which was significantly different from that of WT at 26.11 μm (Figure 2F,G). Meanwhile, the number of stoma was increased, especially that of the adaxial leaf epidermis, which was 84 per microscopic view in MIM319, indicating a significant increase compared with the WT (30 per microscopic view) (Figure 2H). A looser arrangement of mesophyll cells (including spongy tissue and palisade tissue) in the leaf transverse section (Figure S4A) and larger intercellular spaces in the petiole transverse section were found compared to that of the WT (Figure S4B).

From the whole plant level, the height of MIM319 was significantly higher than that of WT in the greenhouse (Figure 3A). After transplantation into an incubator for 1 month, the transgenic plants MIM319 were 14.48 cm tall, whereas the WT was only 9.07 cm (Figure 3B). Blocking *IbmiR319a* also led to a decreased stem diameter in the transgenic plant MIM319. The diameter of the basal stem of the transgenic plant MIM319 was 1.987 mm, which was much slenderer than that of WT at 3.62 mm (Figure 3C).

During planting, we found that the stems of MIM319 were more brittle and broke easily. We further determined the lignin content, deposition, and the load capacity of the stems. Under the same grinding conditions, the stem powder of MIM319 was finer than that of WT (Figure 3D,E). Furthermore, the total Klason lignin content of MIM319 was 296.10 $\mu\text{g/gFW}$, which was decreased compared to the 346.45 $\mu\text{g/gFW}$ in WT (Figure 3F). Toluidine blue staining for lignin in the third internodes also revealed a lower number of lignified cells around the xylem, as indicated by the decreased coloration in comparison with the WT (Figure S5A). Less purplish-red staining by saffron was observed in the vertical section of MIM319 stems than that in WT (Figure S5B). The breaking force of MIM319 was 1938 g/mm^2 , which was also significantly less than 4226.67 g/mm^2 in WT (Figure 3G).

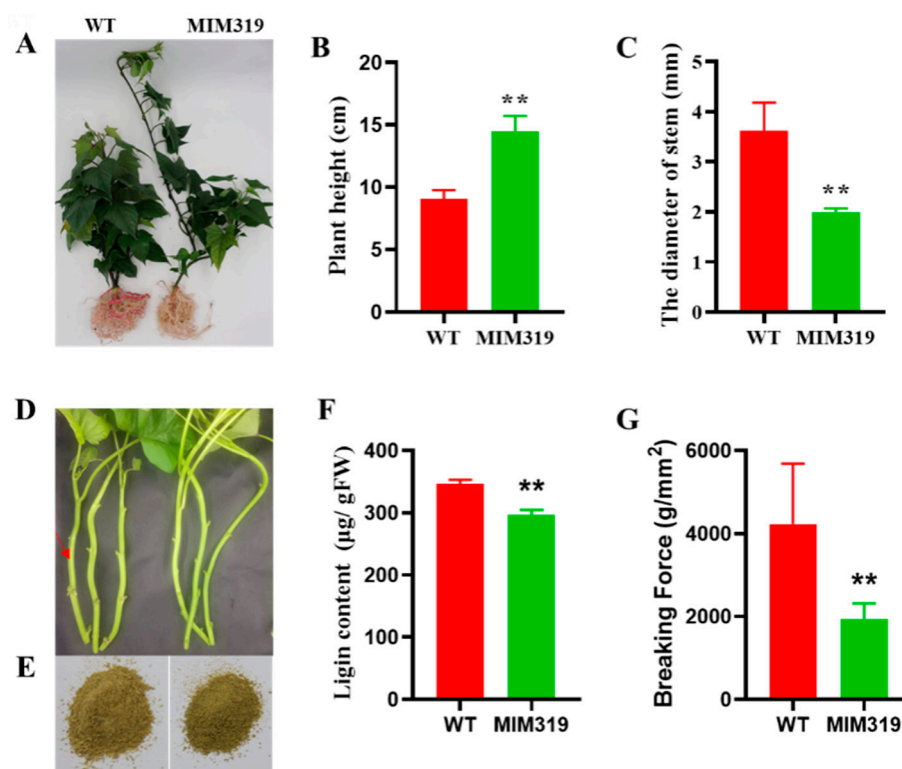


Figure 3. Phenotypes of MIM319 transgenic sweet potato plants. (A): The transgenic plants (MIM319) exhibited an increased plant height and decreased stem diameter compared to the WT controls. (B): Statistical analysis of plant height in MIM319 transgenic plants and WT ($n = 20$). (C): Statistical analysis of stem diameter in MIM319 transgenic plants and WT ($n = 20$). (D): A closer look at the MIM319 transgenic plants and WT. The representative transgenic plant stem is slender. The red arrow indicates the sample location. (E): Powdered stems of MIM319 (left) and WT (right). (F): Statistical analysis of lignin content in WT and MIM319 transgenic plants ($n = 10$). (G): The breaking force of the stems in the WT and MIM319 transgenic plants ($n = 20$). Data are presented as means \pm SE, and error bars represent SE. ** indicate significant differences between transgenic and control plants at $p < 0.01$ by Student's t -test.

All these findings suggest that blocking *IbmiR319a*, with the resulting upregulation of *IbTCP11/17*, caused alterations in the growth and development and lignin content in sweet potato.

3.5. RNA-Seq Analysis of Transgenic Sweet Potato Plants with Blocked *IbmiR319a*

To explore the potential molecular mechanisms affecting the growth and development in MIM319 plants, RNA-Seq analysis was performed using the shoots of the MIM319 lines and WT. The DEGs were identified based on adjusted p -values < 0.05 . To validate the RNA-Seq data, the expression of 10 randomly selected DEGs was examined by qRT-PCR and was found to be consistent with that determined by RNA-Seq (Figure S6). The RNA-Seq results identified 5587 DEGs between MIM319 and WT plants, including 3119 upregulated and 2468 downregulated genes (Figure 4A, Supplementary Table S2). The GO functional annotation of the DEGs revealed that blocking *IbmiR319a* affected multiple biological processes, including the developmental process, growth, metabolic process, and signal transduction (Figure 4B, Supplementary Table S3). The KEGG pathway analysis showed that 116 DEGs were enriched in MAPK signaling transduction, and 80 DEGs were enriched in phenylpropanoid biosynthesis (Figure 4C, Supplementary Table S4). For example, the transcript CL5843.Contig1_Ib, which is homologous to longifolia1-like, functions in regulating leaf morphology by promoting cell expansion in the leaf-length direction [46,47]. The mutant of transcript CL431.Contig8_Ib, which is homologous to E3 ubiquitin-protein

ligase DIS1, was defective in trichome cell expansion and actin organization, resulting in a distorted trichome phenotype [48] in *Arabidopsis*. Transcript CL11749.Contig1_Ib, defined as a SAUR family protein, plays a central role in auxin-induced acid growth [49,50].

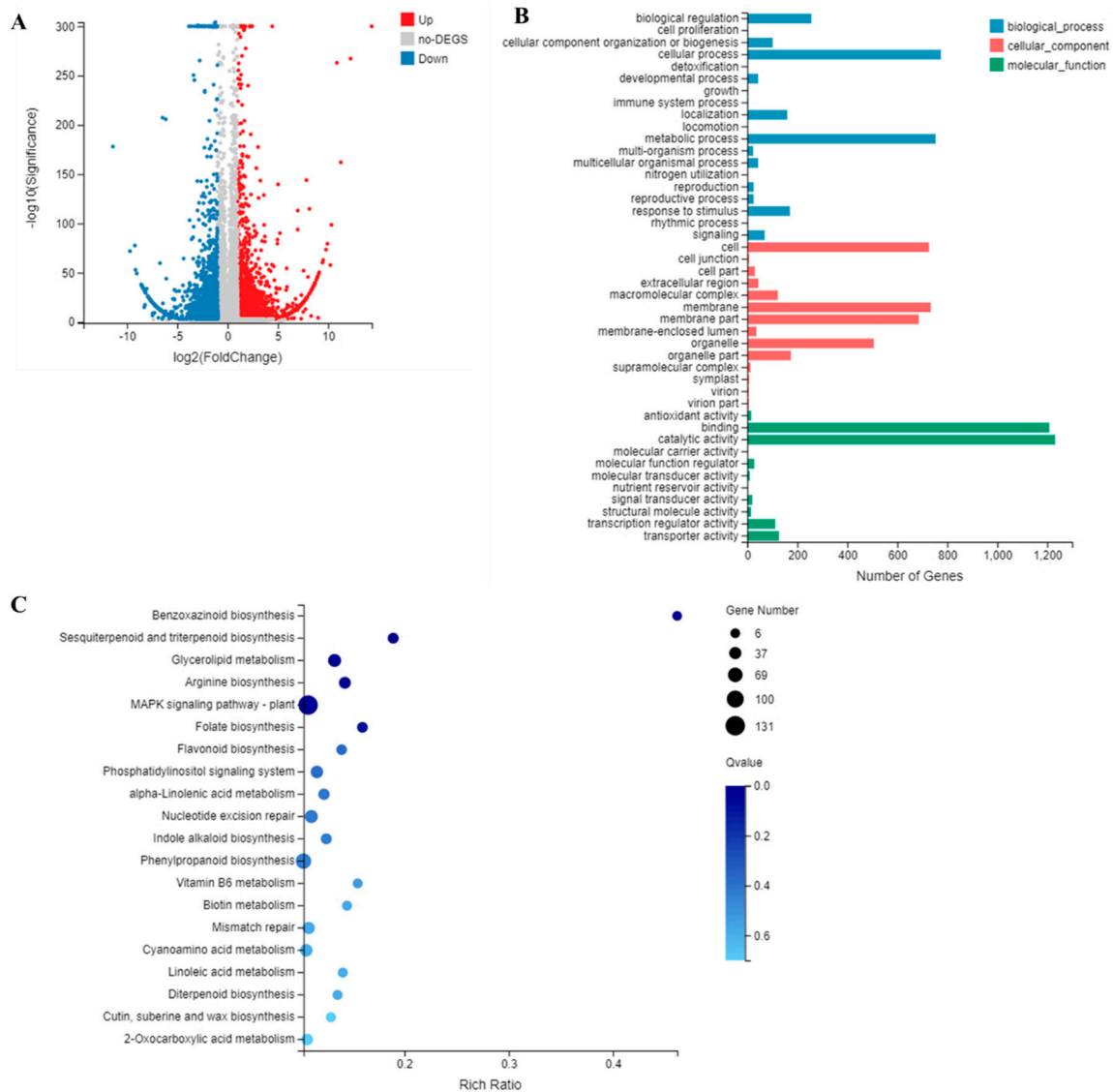


Figure 4. RNA-Seq analysis of MIM319 transgenic sweet potato and WT. (A): Volcano plot shows the differentially expressed genes (DEGs) between MIM319 transgenic sweet potato and WT. Blue circles represent downregulated DEGs; red circles represent upregulated DEGs; and grey circles represent non-DEGs. (B): GO analysis of the DEGs between MIM319 transgenic sweet potato and WT. (C): KEGG pathway analysis of the DEGs between MIM319 transgenic sweet potato and WT.

3.6. Transgenic *Arabidopsis* Plants Overexpressing *IbTCP11* and *IbTCP17* Also Had a Narrow and Small Leaf Phenotype and Decreased Lignin Content

To further examine the function of *IbmiR319a*, a biological function analysis of *IbTCP11* and *IbTCP17* was conducted. We individually overexpressed each of these two genes in *Arabidopsis*. Transgenic *Arabidopsis* plants overexpressing *IbTCP11* (*IbTCP11OE*) and *IbTCP17* (*IbTCP17OE*) had narrow and small leaves, a decreased number of rosette leaves (Figure 5A,B), and a decreased lignin content (Figure 5C), and also resembled the MIM319 phenotype in sweet potato, in which *IbTCP11/17* was upregulated because of native *IbmiR319a* being blocked. The expression profile of these two target genes in various tissues was examined by qRT-PCR in our previous study [45]. *IbTCP11/17* was highly expressed in

the aboveground tissues, including the shoot bud, leaf, and stem, but weakly expressed in the belowground organs. The expression level of *IbTCP11/17* was relatively negatively correlated with the expression of *IbmiR319a*, at least in the shoot buds and leaves. These results suggest that these two target genes *IbTCP11/17* might be involved in the regulation of plant architecture and lignin content.

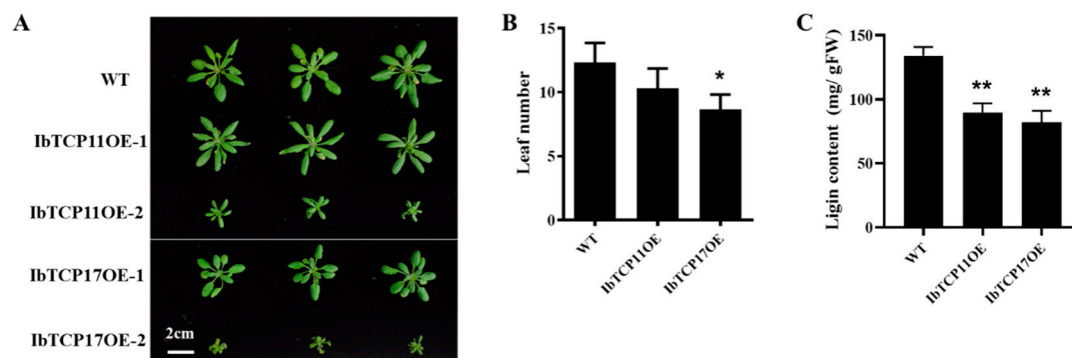


Figure 5. Phenotypes of transgenic *Arabidopsis* plants. (A): The transgenic plants (IbTCP11-OE and IbTCP17-OE) exhibited a smaller plant structure and leaf to the WT controls. Photographs of representative seedlings of WT and two transgenic lines were taken. (B): Leaf number in IbTCP11OE and IbTCP17OE transgenic plants and WT ($n = 20$). (C): Lignin content in IbTCP11-OE and IbTCP17-OE transgenic plants and WT ($n = 10$). *, ** indicate significant differences between transgenic and control plants at $p < 0.05$, 0.01.

3.7. Blocking *IbmiR319a* in Sweet Potato Resulted in Decreased Drought Tolerance

We wanted to assess whether blocking *IbmiR319a* would affect the performance of sweet potato under drought conditions due to morphological changes in the stems and leaves. MIM319 and WT plants with 3–4 mature leaves were subjected to drought for 4 weeks. All plants showed wilting, yellowing, and necrosis, although the leaves of MIM319 showed more severe withering than those of WT. After re-watering for two weeks, most WT plants survived while the MIM319 transgenic plants perished (Figure 6A).

The drought tolerance of the plants was further evaluated. No differences in the MDA contents between the MIM319 transgenic plants and WT were observed under control conditions (room temperature or normal watering). However, the MDA content of MIM319 increased by 2.65 and 2.9 times, respectively, under drought stress compared to normal conditions, whereas an increase of only 1.97 times was detected in WT (Figure 6B).

An opposite pattern was observed for the proline content. There was no difference in the proline contents between the MIM319 transgenic plants and WT under control conditions. By contrast, under drought treatment, the proline content of MIM319 was significantly increased by 1.77 and 1.94 times, respectively, which were all lower than the 2.3 times increase detected in WT (Figure 6B).

Quantitative RT-PCR analysis was also used to detect the expression level of the drought stress-responsive genes. Well-known stress-responsive genes, including a proline biosynthesis-related gene encoding a pyrroline-5-carboxylatesynthase (*IbP5CS*) and pyrroline-5-carboxylate reductase (*IbP5CR*); an abscisic acid (ABA) biosynthesis-related gene encoding a zeaxanthin epoxidase (*IbZEP*); 9-*cis*-epoxycarotenoid dioxygenase (*IbNCED*); a late embryogenesis abundant protein (*IbLEA*); a photosynthesis-related gene encoding a phosphoribulokinase (*IbPRK*); and ROS scavenging-related genes encoding superoxide dismutase (*IbSOD*), peroxidase (*IbPOD*), catalase (*IbCAT*), ascorbate peroxidase (*IbAPX*), and glutathione peroxidase (*IbGPX*), were significantly downregulated in the MIM319 transgenic plants compared to WT after two weeks of drought stress (Figure 6C,D).

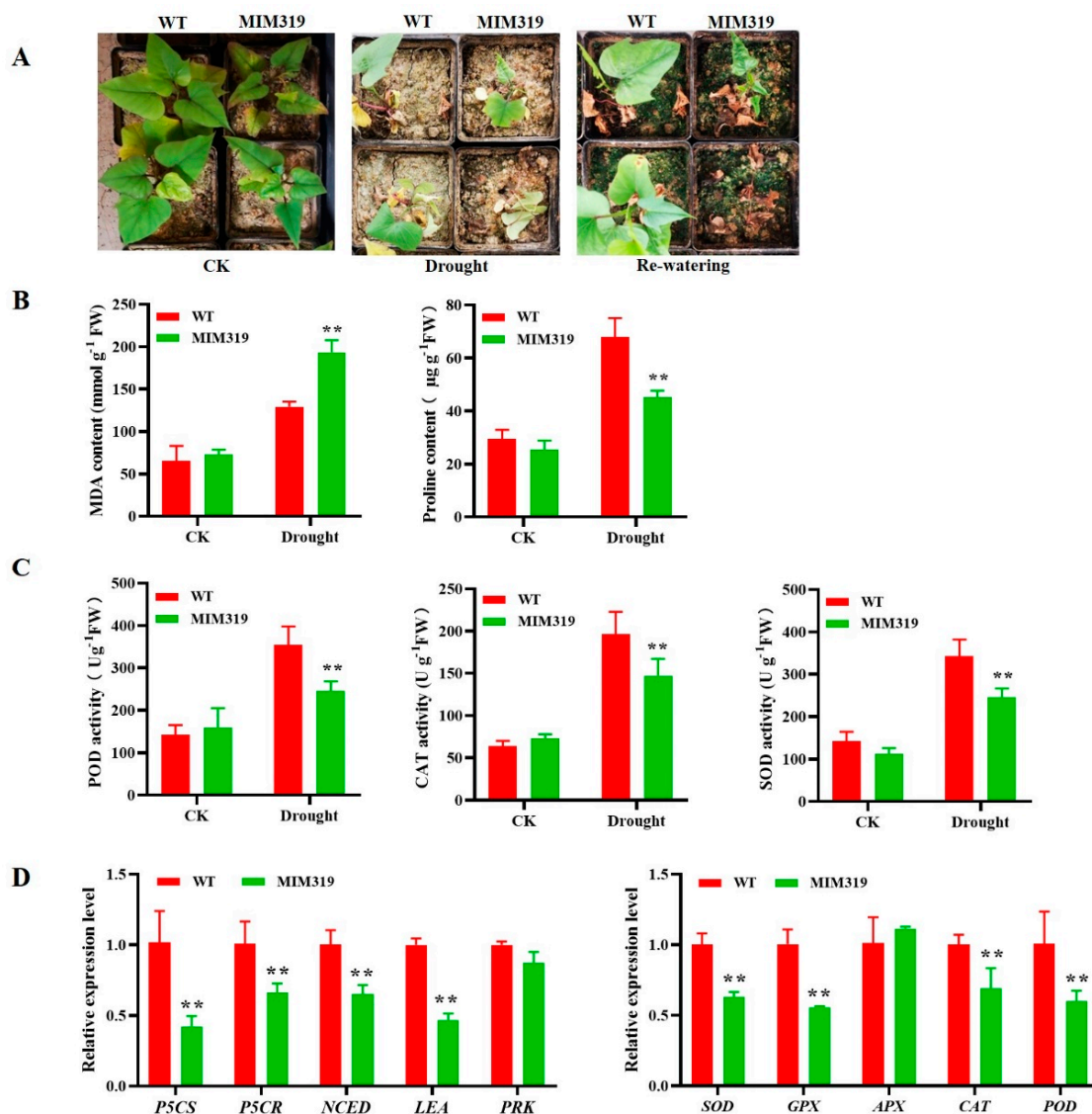


Figure 6. Drought tolerance analysis of MIM319 transgenic sweet potato plants. (A): Phenotypes of MIM319 transgenic plants vs. WT grown for 6 weeks under normal conditions (CK) and 4 weeks under drought stress (Drought) followed by 2 days of re-watering after 2 weeks of normal treatment (Re-watering). (B): MDA and proline contents in the MIM319 transgenic plants and WT grown for 2 weeks under drought stress after 2 weeks of normal treatment. (C): Peroxidase (POD), catalase (CAT), and superoxide dismutase (SOD) activity in the MIM319 transgenic plants and WT grown for 2 weeks under drought stress after 2 weeks of normal treatment. (D): Transcript levels of salt and drought-responsive genes in the leaves of MIM319 transgenic plants and WT plants that had been pot-grown for 4 weeks under normal conditions and 2 weeks under drought stress after 2 weeks of normal treatment. Each value is the mean of three biological repeats \pm the standard deviation (SD). ** indicate significant differences between transgenic lines and WT. $p < 0.01$, Student's t -test.

These results implied that blocking *IbmiR319a* inhibited the antioxidant system, which includes the inhibited transcriptional expression and the activity of the ROS-scavenging enzymes under drought stress.

3.8. *IbmiR319a* Functions in Plant Tolerance of Drought Stress Possibly by Inhibiting *IbTCP11/17* Expression in Sweet Potato

The expression level of *IbTCP11/17* in the WT sweet potato was more strongly induced by polyethylene glycol (PEG) 6000, which was used to simulate drought stress. The

expression of *IbTCP11* peaked (2 times) at 12 h while that of *IbTCP17* peaked (6 times) at 6 h (Figure 7A,B). These results implied that *IbTCP11/17* might be involved in drought tolerance in sweet potato. To further confirm this, the expression level of *IbTCP11/17* responding to water withdrawal was also detected. The expression of *IbTCP11* peaked at 4 days while that of *IbTCP17* peaked at 7 days after water withdrawal (Figure 7C,D). These results confirmed that the target genes *IbTCP11/17* were indeed involved in drought tolerance in sweet potato.

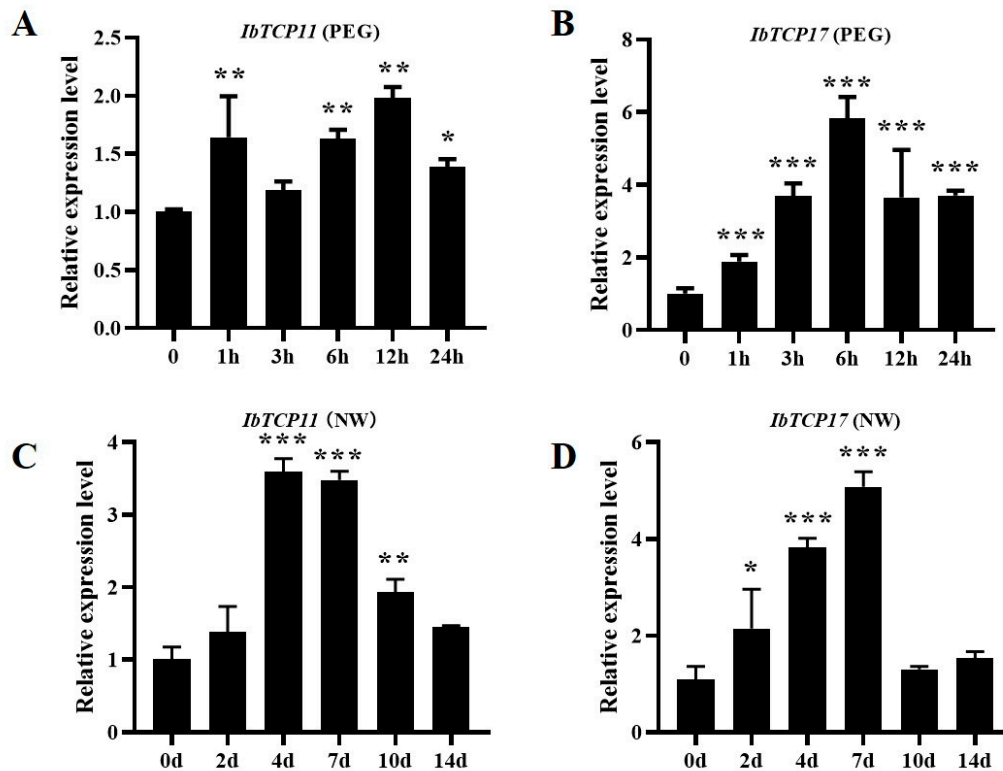


Figure 7. Expression analysis of the target genes *IbTCP11* and *IbTCP17* responding to drought. (A): Expression level of *IbTCP11* in the WT at different times (h) in response to 20% PEG. (B): Expression level of *IbTCP17* in the WT at different times (h) in response to 20% PEG. (C): Expression level of *IbTCP11* in the WT at different times (d) in response to drought stress with no water (NW). (D): Expression level of *IbTCP17* in the WT at different times (d) in response to drought stress with no water. Data are presented as mean values \pm SE ($n = 3$). * and **, *** indicate a significant difference compared to the WT at $p < 0.05$ and < 0.01 , < 0.001 , respectively, based on Student's t -test.

4. Discussion

Although sweet potato is a root crop that is highly important for food security [51], research on sweet potato has lagged behind other crops, such as rice, wheat, and maize, because of the complexity of the genome and the inefficiency of genetic transformation. So far, the only functionally characterized miRNAs in sweet potato are *IbmiR2111* [52], *IbmiR828* [53], and *IbmiR408* [54]. In the present study, we found that *IbmiR319a* negatively regulated the abundance of *IbTCP11/17* mRNA, which affected plant architecture and drought tolerance in sweet potato.

In sweet potato, the miR319 family has two members that are each encoded by *IbMIR319a* and *IbMIR319c*. A growing number of studies have reported that the function of miR319 is far ranging and conserved among different species [6,33,34,37,55]. The overexpression of *miR319* or downregulation of its target genes leads to a broader and crinkled leaf phenotype in transgenic dicotyledonous plants, such as *Arabidopsis* [28], and tomato [37], but only a broader leaf phenotype in transgenic monocotyledonous plants, such as rice [31] and switchgrass [56]. In our study, blocking *IbmiR319a* led to a narrow and small leaf phenotype in transgenic sweet potato, which was the opposite phenotype to the overexpression

transgenic plant. Blocking *IbmiR319a* also led to a decreased stem diameter in transgenic plants. These results suggest that the function of miR319 in leaf morphogenesis and plant growth is highly conserved in sweet potato. In addition, we found that ~5000 genes were differentially expressed in MIM319 (Figure 4), which suggested that *IbmiR319* plays a global regulatory role in the multiple biological processes of sweet potato.

AtTCP2, an orthologous gene of *IbTCP11*, interacts with *AtCRY1* to inhibit hypocotyl elongation under blue light [57]. The function of *CsnTCP2* was shown to be suppressed by *CsnmiR319c* in the bud dormancy-activity cycle in tea plant [33]. *AtTCP2* also positively regulated the expression of *Circadian clock associated 1 (CCA1)* and *EARLY FLOWERING 3 (ELF3)* to affect leaf morphogenesis and flowering time and mediate the jasmonic acid (JA) signaling pathway to inhibit hypocotyl elongation [58]. *AtTCP4*, an orthologous gene of *IbTCP17*, directly activates *VND7* to participate in secondary cell wall biosynthesis and programmed cell death [59], and also directly activates *TRICHOMELESS1 (TCL1)* and *TCL2* to suppress trichome initiation [60]. *AtTCP4* and *PIF3* antagonistically participate in photomorphogenesis and facilitate light-induced cotyledon opening in *Arabidopsis* [61]. Among the 18 *IbTCP* genes in sweet potato, there are only 4 complementarily targeted by *IbmiR319* [45]. Overexpression of the target genes *IbTCP11/17* in *Arabidopsis* (*IbTCP11OE*, *IbTCP17OE*) led to a narrow and small leaf phenotype and a decreased lignin content, which was consistent with that of MIM319 in sweet potato.

Leaves are not only important photosynthetic plant organs but are also the interface for plant water metabolism [62]. Water loss through stomatal transpiration is one of the key determinants of drought tolerance [63]. The density and distribution of stomata directly affect plant water metabolism and drought tolerance. In our study, the leaf epidermal cells were slenderer and had more stomata in MIM319 than in WT, and the mesophyll cells were more loosely arranged, and the intercellular space was larger in MIM319 than in WT, all of which may result in increased water loss and decreased drought tolerance.

Reactive oxygen species (ROS) can cause damage to the structure and function of biomolecules, which leads to oxidative stress in plants. MDA as one of the prominent ROS, is the final decomposition product of membrane lipid peroxidation and its content can reflect the degree of plant damage by various stresses. Proline is another essential member of ROS, and its accumulation can protect plants against ROS damage. In this study, we found that the MDA content increased much more in MIM319 than WT while the proline content decreased (Figure 6B). In addition, the ROS-scavenging system genes, including *IbSOD*, *IbGPX*, *IbAPX*, *IbCAT*, and *IbPOD*, were downregulated in MIM319 (Figure 6D). These results suggest that blocking miR319 decreases proline accumulation and inactivates the ROS-scavenging system, which leads to reduced drought tolerance in transgenic MIM319.

Lignin is an important polymer of phenylpropanoid compounds and plays a vital role in biotic and abiotic stress tolerance in plants. Greater lignification improves drought resistance by increasing the water retention capacity [64,65]. The overexpression of a rice HD-Zip transcription factor *OsTFIL* [66], foxtail millet (*Setaria italica*) R2R3-MYB transcription factor *SiMYB56* [67], or key genes in the lignin biosynthesis pathway, such as the 4-coumarate-CoA ligases gene in *Gossypium hirsutum* (*Gh4CL7*) [68], cinnamyl alcohol dehydrogenase gene in *Cucumis melo* L. (*CmCAD*) [69], and caffeoyl-CoA O-methyltransferase gene in *Paeonia ostii* (*PoCCoAOMT*) [70], can all significantly enhance tolerance to drought stress in transgenic plants by regulating lignin biosynthesis. In *Arabidopsis*, miR319-targeted *AtTCP4* activated *VND7* expression to increase the lignin content in the secondary cell wall [59]. In our study, blocking *IbmiR319a* led to increased brittleness and a decreased lignin content, and as a result, reduced the drought tolerance in sweet potato.

In summary, we demonstrated that miR319 from sweet potato, targeting transcription factors *IbTCP11* and *IbTCP17*, is involved in plant architecture and drought tolerance. Blocking *IbmiR319*, upregulating the expression of *IbTCP11* and *IbTCP17*, caused a slim and tender phenotype and greater sensitivity to drought stress. This study provides a novel miR319 gene for impacting plant architecture drought tolerance of sweet potato.

Supplementary Materials: The following supporting information can be downloaded at: <https://www.mdpi.com/article/10.3390/genes13030404/s1>, Figure S1: The results of blasting the IbmiR319a precursor and IbmiR319c precursor in the sweet potato public database. Figure S2: The detection of MIM319 transgenic sweet potato. Figure S3: The results of the blast search of the target genes *IbTCP11* and *IbTCP17* in the genomics database of the two wild ancestors (*I. trifida* and *I. triloba*) of sweet potato. Figure S4: Microscopic analysis of the leaf transverse paraffin section and petiole transverse freehand section in MIM319 transgenic sweet potato and WT. Figure S5: Lignin deposition patterns in the stem of the third internode freehand transverse section staining with toluidine blue (TB) and vertical paraffin section staining with Safranin O-Fast Green. Figure S6: Validation of the transcriptome sequencing results. Table S1: Primers used in this study. Table S2: List of the differentially expressed genes (DEGs) between MIM319 transgenic sweet potato and WT. Table S3: GO analysis of DEGs. Table S4: KEGG pathway enrichment analysis.

Author Contributions: L.R., Z.L., D.M. and A.W. designed the research. L.R., T.Z., H.W. (Haixia Wu), X.G. and H.W. (Huihui Wan) performed the experiments. S.C. contributed to planting. Z.L. contributed to reagents, materials, and analysis tools. L.R. and A.W. wrote the manuscript. Z.L. and D.M. modified the manuscript. All authors have read and agreed to the published version of the manuscript.

Funding: This work was supported by the China Agriculture Research System of MOF and MARA (Grant No. CARS-10-B02), the National Key R&D Program of China (2018YFD1000705 and 2018YFD1000700), the Project of Xuzhou Science and Technology Key R&D Program (Grant No. KC21142), Postgraduate Research & Practice Innovation Program of Jiangsu Province (Grant No. KYCX21_2605), and the Research Innovation Program for College Graduates of Jiangsu Normal University (Grant No. 2020XKT497; 2021XKT0785), the Priority Academic Program Development of Jiangsu Higher Education Institutions (PAPD).

Institutional Review Board Statement: Not applicable.

Informed Consent Statement: Not applicable.

Conflicts of Interest: The authors declare no conflict of interest.

References

- Pearce, R.S. Plant freezing and damage. *Ann. Bot.* **2001**, *87*, 417–424. [[CrossRef](#)]
- Xie, Z.; Wang, A.; Li, H.; Yu, J.; Jiang, J.; Tang, Z.; Ma, D.; Zhang, B.; Han, Y.; Li, Z. High throughput deep sequencing reveals the important roles of microRNAs during sweetpotato storage at chilling temperature. *Sci. Rep.* **2017**, *7*, 16578. [[CrossRef](#)] [[PubMed](#)]
- Meng, X.Q.; Li, G.; Yu, J.; Cai, J.; Dong, T.T.; Sun, J.; Xu, T.; Li, Z.Y.; Pan, S.Y.; Ma, D.F.; et al. Isolation, Expression Analysis, and Function Evaluation of 12 Novel Stress-Responsive Genes of NAC Transcription Factors in Sweetpotato. *Crop Sci.* **2018**, *58*, 1328–1341. [[CrossRef](#)]
- Burke, M.B.; Lobell, D.B.; Guarino, L. Shifts in African crop climates by 2050, and the implications for crop improvement and genetic resources conservation. *Glob. Environ. Chang.* **2009**, *19*, 317–325. [[CrossRef](#)]
- Hu, H.; Xiong, L. Genetic engineering and breeding of drought-resistant crops. *Annu. Rev. Plant Biol.* **2014**, *65*, 715–741. [[CrossRef](#)]
- Zhou, M.; Li, D.; Li, Z.; Hu, Q.; Yang, C.; Zhu, L.; Luo, H. Constitutive expression of a miR319 gene alters plant development and enhances salt and drought tolerance in transgenic creeping bentgrass. *Plant Physiol.* **2014**, *161*, 1375–1391. [[CrossRef](#)]
- Lin, K.H.; Chiang, C.M.; Lai, Y.C.; You, S.H.; Lo, H.F. Identification of Chilling-inducible Genes in Sweet potato by Suppression Subtractive Hybridization. *Res. J. Biotechnol.* **2011**, *6*, 37–43.
- Sato, Y.; Murakami, T.; Funatsuki, H.; Matsuba, S.; Saruyama, H.; Tanida, M. Heat shock-mediated APX gene expression and protection against chilling injury in rice seedlings. *J. Exp. Bot.* **2001**, *52*, 145. [[CrossRef](#)]
- Motsa, N.M.; Modi, A.T.; Mabhaudhi, T. Sweet potato (*Ipomoea batatas* L.) as a drought tolerant and food security crop. *S. Afr. J. Sci.* **2005**, *111*, 11–12. [[CrossRef](#)]
- Mbinda, W.; Dixelius, C.; Oduor, R. Induced Expression of Xerophyta viscosa XvSap1 Gene Enhances Drought Tolerance in Transgenic Sweet Potato. *Front. Plant Sci.* **2019**, *10*, 1119. [[CrossRef](#)]
- Fan, W.; Zhang, M.; Zhang, H.; Zhang, P. Improved tolerance to various abiotic stresses in transgenic sweet potato (*Ipomoea batatas*) expressing spinach betaine aldehyde dehydrogenase. *PLoS ONE* **2012**, *7*, e37344. [[CrossRef](#)] [[PubMed](#)]
- Ruan, L.; Chen, L.J.; Chen, Y.H.; He, J.L.; Zhang, W.; Gao, Z.L.; Zhang, Y.H. Expression of Arabidopsis HOMEODOMAIN GLABROUS 11 Enhances Tolerance to Drought Stress in Transgenic Sweet Potato Plants. *J. Plant Biol.* **2011**, *55*, 151–158. [[CrossRef](#)]
- Mbinda, W.; Ombori, O.; Dixelius, C.; Oduor, R. Xerophyta viscosa Aldose Reductase, XvAld1, Enhances Drought Tolerance in Transgenic Sweetpotato. *Mol. Biotechnol.* **2018**, *60*, 203–214. [[CrossRef](#)] [[PubMed](#)]

14. Wang, A.M.; Zhu, M.K.; Luo, Y.H.; Liu, Y.J.; Li, R.S.; Kou, M.; Wang, X.; Zhang, Y.G.; Meng, X.Q.; Zheng, Y.L.; et al. A sweet potato cinnamate 4-hydroxylase gene, IbC4H, increases phenolics content and enhances drought tolerance in tobacco. *Acta Physiol. Plant* **2017**, *39*, 276. [[CrossRef](#)]
15. Zhai, H.; Wang, F.; Si, Z.; Huo, J.; Xing, L.; An, Y.; He, S.; Liu, Q. A myo-inositol-1-phosphate synthase gene, IbMIPS1, enhances salt and drought tolerance and stem nematode resistance in transgenic sweet potato. *Plant Biotechnol. J.* **2016**, *14*, 592–602. [[CrossRef](#)]
16. Jin, R.; Kim, B.H.; Ji, C.Y.; Kim, H.S.; Li, H.M.; Ma, D.F.; Kwak, S.S. Overexpressing IbCBF3 increases low temperature and drought stress tolerance in transgenic sweetpotato. *Plant Physiol. Biochem.* **2017**, *118*, 45–54. [[CrossRef](#)]
17. Wang, B.; Zhai, H.; He, S.Z.; Zhang, H.; Ren, Z.T.; Zhang, D.D.; Liu, Q.C. A vacuolar Na⁺/H⁺ antiporter gene, IbNHX2, enhances salt and drought tolerance in transgenic sweetpotato. *Sci. Hortic.* **2016**, *201*, 153–166. [[CrossRef](#)]
18. Zhou, Y.; Zhai, H.; He, S.; Zhu, H.; Gao, S.; Xing, S.; Wei, Z.; Zhao, N.; Liu, Q. The Sweetpotato BTB-TAZ Protein Gene, IbBT4, Enhances Drought Tolerance in Transgenic *Arabidopsis*. *Front. Plant Sci.* **2020**, *11*, 877. [[CrossRef](#)]
19. Kang, C.; He, S.; Zhai, H.; Li, R.; Zhao, N.; Liu, Q. A Sweetpotato Auxin Response Factor Gene (IbARF5) Is Involved in Carotenoid Biosynthesis and Salt and Drought Tolerance in Transgenic *Arabidopsis*. *Front. Plant Sci.* **2018**, *9*, 1307. [[CrossRef](#)]
20. Kang, C.; Zhai, H.; He, S.; Zhao, N.; Liu, Q. A novel sweetpotato bZIP transcription factor gene, IbZIP1, is involved in salt and drought tolerance in transgenic *Arabidopsis*. *Plant Cell Rep.* **2019**, *38*, 1373–1382. [[CrossRef](#)]
21. Wang, W.; Qiu, X.; Yang, Y.; Kim, H.S.; Jia, X.; Yu, H.; Kwak, S.S. Sweetpotato bZIP Transcription Factor IbABF4 Confers Tolerance to Multiple Abiotic Stresses. *Front. Plant Sci.* **2019**, *10*, 630. [[CrossRef](#)] [[PubMed](#)]
22. Zhou, Y.; Zhu, H.; He, S.; Zhai, H.; Zhao, N.; Xing, S.; Wei, Z.; Liu, Q. A Novel Sweetpotato Transcription Factor Gene IbMYB116 Enhances Drought Tolerance in Transgenic *Arabidopsis*. *Front. Plant Sci.* **2019**, *10*, 1025. [[CrossRef](#)] [[PubMed](#)]
23. Schommer, C.; Palatnik, J.F.; Aggarwal, P.; Chételat, A.; Cubas, P.; Farmer, E.E.; Nath, U.; Weigel, D. Control of jasmonate biosynthesis and senescence by miR319 targets. *PLoS Biol.* **2008**, *6*, e230. [[CrossRef](#)] [[PubMed](#)]
24. Chen, X. Small RNAs and their roles in plant development. *Annu. Rev. Cell Dev. Biol.* **2009**, *1*, 21–44. [[CrossRef](#)]
25. Taylor, R.S.; Tarver, J.E.; Hiscock, S.J.; Donoghue, P.C. Evolutionary history of plant microRNAs. *Trends Plant Sci.* **2014**, *19*, 175–182. [[CrossRef](#)]
26. Axtell, M.J.; Snyder, J.A.; Bartel, D.P. Common Functions for Diverse Small RNAs of Land Plants. *Plant Cell* **2007**, *19*, 1750–1769. [[CrossRef](#)]
27. Sunkar, R.; Zhu, J.K. Novel and Stress-Regulated MicroRNAs and Other Small RNAs from *Arabidopsis*. *Plant Cell* **2004**, *16*, 2001–2019. [[CrossRef](#)]
28. Palatnik, J.F.; Allen, E.; Wu, X.; Schommer, C.; Schwab, R.; Carrington, J.C.; Weigel, D. Control of leaf morphogenesis by microRNAs. *Nature* **2003**, *425*, 257–263. [[CrossRef](#)]
29. Jones-Rhoades, M.W.; Bartel, D.P.; Bartel, B. MicroRNAs and their regulatory roles in plants. *Annu. Rev. Plant Biol.* **2006**, *57*, 19–53. [[CrossRef](#)]
30. Schommer, C.; Debernardi, J.M.; Bresso, E.G.; Rodriguez, R.E.; Palatnik, J.F. Repression of Cell Proliferation by miR319-Regulated TCP4. *Mol. Plant* **2014**, *7*, 1533–1544. [[CrossRef](#)]
31. Yang, C.; Li, D.; Mao, D.; Liu, X.; Ji, C.; Li, X.; Zhao, X.; Cheng, Z.; Chen, C.; Zhu, L. Overexpression of microRNA319 impacts leaf morphogenesis and leads to enhanced cold tolerance in rice (*Oryza sativa* L.). *Plant Cell Environ.* **2013**, *36*, 2207–2218. [[CrossRef](#)]
32. Wang, S.T.; Sun, X.L.; Hoshino, Y.; Yu, Y.; Jia, B.; Sun, Z.W.; Sun, M.Z.; Duan, X.B.; Zhu, Y.M. MicroRNA319 positively regulates cold tolerance by targeting OsPCF6 and OsTCP21 in rice (*Oryza sativa* L.). *PLoS ONE* **2014**, *9*, e91357. [[CrossRef](#)] [[PubMed](#)]
33. Liu, S.; Mi, X.; Zhang, R.; An, Y.; Zhou, Q.; Yang, T.; Xia, X.; Guo, R.; Wang, X.; Wei, C. Integrated analysis of miRNAs and their targets reveals that miR319c/TCP2 regulates apical bud burst in tea plant (*Camellia sinensis*). *Planta* **2019**, *250*, 1111–1129. [[CrossRef](#)] [[PubMed](#)]
34. Fan, D.; Ran, L.; Hu, J.; Ye, X.; Xu, D.; Li, J.; Su, H.; Wang, X.; Ren, S.; Luo, K. miR319a/TCP module and DELLA protein regulate trichome initiation synergistically and improve insect defenses in *Populus tomentosa*. *New Phytol.* **2020**, *227*, 867–883. [[CrossRef](#)]
35. Wang, F.L.; Zheng, T.; Wu, G.T.; Lang, C.X.; Hu, Z.H.; Shi, J.H.; Wei, J.; Chen, J.Q.; Liu, R.H. Overexpression of miR319a Affects the Balance between Mitosis and Endoreduplication in *Arabidopsis* Leaves. *Plant Mol. Biol. Rep.* **2015**, *33*, 2006–2013. [[CrossRef](#)]
36. Chen, H.; Rosin, F.M.; Prat, S.; Hannapel, D.J. Interacting transcription factors from the three-amino acid loop extension superclass regulate tuber formation. *Plant Physiol.* **2003**, *132*, 1391–1404. [[CrossRef](#)] [[PubMed](#)]
37. Shi, X.; Jiang, F.; Wen, J.; Wu, Z. Overexpression of *Solanum habrochaites* microRNA319d (sha-miR319d) confers chilling and heat stress tolerance in tomato (*S. lycopersicum*). *BMC Plant Biol.* **2019**, *19*, 214. [[CrossRef](#)]
38. Liu, Y.; Li, D.; Yan, J.; Wang, K.; Zhang, W. MiR319-mediated ethylene biosynthesis, signalling and salt stress response in switchgrass. *Plant Biotechnol. J.* **2019**, *17*, 2370–2383. [[CrossRef](#)]
39. Franco-Zorrilla, J.M.; Valli, A.; Todesco, M.; Mateos, I.; Puga, M.I.; Rubio-Somoza, I.; Leyva, A.; Weigel, D.; Garcia, J.A.; Paz-Ares, J. Target mimicry provides a new mechanism for regulation of microRNA activity. *Nat. Genet.* **2007**, *39*, 1033–1037. [[CrossRef](#)]
40. Yang, J.; Bi, H.P.; Fan, W.J.; Zhang, M.; Wang, H.X.; Zhang, P. Efficient embryogenic suspension culturing and rapid transformation of a range of elite genotypes of sweet potato (*Ipomoea batatas* [L.] Lam.). *Plant Sci.* **2011**, *181*, 701–711. [[CrossRef](#)]
41. Clough, S.J.; Bent, A.F. Floral dip: A simplified method for *Agrobacterium*-mediated transformation of *Arabidopsis thaliana*. *Plant J.* **1998**, *16*, 735–743. [[CrossRef](#)] [[PubMed](#)]

42. Livak, K.J.; Schmittgen, T.D. Analysis of relative gene expression data using real-time quantitative PCR and the 2(-Delta Delta C(T)) Method. *Methods* **2001**, *25*, 402–408. [[CrossRef](#)] [[PubMed](#)]
43. Hatfield, R.D.; Jung, H.J.G.; Ralph, J.; Buxton, D.R.; Weimer, P.J. A comparison of the insoluble residues produced by the Klason lignin and acid detergent lignin procedures. *J. Sci. Food Agric.* **2010**, *65*, 51–58. [[CrossRef](#)]
44. Abdi, H. The Bonferonni and Šidák Corrections for Multiple Comparisons. *Encycl. Meas. Stat.* **2007**, *1*, 1–9.
45. Ren, L.; Wu, H.; Zhang, T.; Ge, X.; Wang, T.; Zhou, W.; Zhang, L.; Ma, D.; Wang, A. Genome-Wide Identification of TCP Transcription Factors Family in Sweet Potato Reveals Significant Roles of miR319-Targeted TCPs in Leaf Anatomical Morphology. *Front. Plant Sci.* **2021**, *12*, 686698. [[CrossRef](#)]
46. Lee, Y.K.; Kim, G.T.; Kim, I.J.; Park, J.; Kwak, S.S.; Choi, G.; Chung, W.I. LONGIFOLIA1 and LONGIFOLIA2, two homologous genes, regulate longitudinal cell elongation in *Arabidopsis*. *Development* **2006**, *133*, 4305–4314. [[CrossRef](#)]
47. Lee, Y.K.; Kim, I.J. Functional conservation of *Arabidopsis* LNG1 in tobacco relating to leaf shape change by increasing longitudinal cell elongation by overexpression. *Genes Genom.* **2018**, *40*, 1053–1062. [[CrossRef](#)]
48. Zou, J.J.; Zheng, Z.Y.; Xue, S.; Li, H.H.; Wang, Y.R.; Le, J. The role of *Arabidopsis* Actin-Related Protein 3 in amyloplast sedimentation and polar auxin transport in root gravitropism. *J. Exp. Bot.* **2016**, *67*, 5325–5337. [[CrossRef](#)]
49. Stortenbeker, N.; Bemer, M. The SAUR gene family: The plant's toolbox for adaptation of growth and development. *J. Exp. Bot.* **2019**, *70*, 17–27. [[CrossRef](#)]
50. Wang, J.; Sun, N.; Zhang, F.; Yu, R.; Chen, H.; Deng, X.W.; Wei, N. SAUR17 and SAUR50 Differentially Regulate PP2C-D1 during Apical Hook Development and Cotyledon Opening in *Arabidopsis*. *Plant Cell* **2002**, *32*, 3792–3811. [[CrossRef](#)]
51. Liu, Q.; Liu, J.; Zhang, P.; He, S. *Root and Tuber Crops*; Encyclopedia of Agriculture and Food Systems; Elsevier: Amsterdam, The Netherlands, 2014; pp. 46–61.
52. Weng, S.T.; Kuo, Y.W.; King, Y.C.; Lin, H.H.; Tu, P.Y.; Tung, K.S.; Jeng, S.T. Regulation of microRNA2111 and its target IbFBK in sweet potato on wounding. *Plant Sci.* **2020**, *292*, 110391. [[CrossRef](#)] [[PubMed](#)]
53. Lin, J.S.; Lin, C.C.; Lin, H.H.; Chen, Y.C.; Jeng, S.T. MicroR828 regulates lignin and H₂O₂ accumulation in sweet potato on wounding. *New Phytol.* **2012**, *196*, 427–440. [[CrossRef](#)] [[PubMed](#)]
54. Kuo, Y.W.; Lin, J.S.; Li, Y.C.; Jhu, M.Y.; King, Y.C.; Jeng, S.T. MicroR408 regulates defense response upon wounding in sweet potato. *J. Exp. Bot.* **2019**, *70*, 469–483. [[CrossRef](#)] [[PubMed](#)]
55. Cao, J.F.; Zhao, B.; Huang, C.C.; Chen, Z.W.; Zhao, T.; Liu, H.R.; Hu, G.J.; Shangguan, X.X.; Shan, C.M.; Wang, L.J.; et al. The miR319-Targeted GhTCP4 Promotes the Transition from Cell Elongation to Wall Thickening in Cotton Fiber. *Mol. Plant* **2020**, *13*, 1063–1077. [[CrossRef](#)]
56. Xie, Q.; Liu, X.; Zhang, Y.; Tang, J.; Yin, D.; Fan, B.; Zhu, L.; Han, L.; Song, G.; Li, D. Identification and Characterization of microRNA319a and Its Putative Target Gene, PvPCF5, in the Bioenergy Grass Switchgrass (*Panicum virgatum*). *Front. Plant Sci.* **2017**, *8*, 396. [[CrossRef](#)]
57. He, Z.; Zhao, X.; Kong, F.; Zuo, Z.; Liu, X. TCP2 positively regulates HY5/HYH and photomorphogenesis in *Arabidopsis*. *J. Exp. Bot.* **2016**, *67*, 775–785. [[CrossRef](#)]
58. He, Z.; Zhou, X.; Chen, J.; Yin, L.; Zeng, Z.; Xiang, J.; Liu, S. Identification of a consensus DNA-binding site for the TCP domain transcription factor TCP2 and its important roles in the growth and development of *Arabidopsis*. *Mol. Biol. Rep.* **2021**, *48*, 2223–2233. [[CrossRef](#)]
59. Sun, X.; Wang, C.; Xiang, N.; Li, X.; Yang, S.; Du, J.; Yang, Y.; Yang, Y. Activation of secondary cell wall biosynthesis by miR319-targeted TCP4 transcription factor. *Plant Biotechnol. J.* **2017**, *15*, 1284–1294. [[CrossRef](#)]
60. Vadde, B.V.L.; Challa, K.R.; Sunkara, P.; Hegde, A.S.; Nath, U. The TCP4 Transcription Factor Directly Activates TRICHOMELESS1 and 2 and Suppresses Trichome Initiation. *Plant Physiol.* **2019**, *181*, 1587–1599. [[CrossRef](#)]
61. Dong, J.; Sun, N.; Yang, J.; Deng, Z.; Lan, J.; Qin, G.; He, H.; Deng, X.W.; Irish, V.F.; Chen, H.; et al. The Transcription Factors TCP4 and PIF3 Antagonistically Regulate Organ-Specific Light Induction of SAUR Genes to Modulate Cotyledon Opening during De-Etiolation in *Arabidopsis*. *Plant Cell* **2019**, *31*, 1155–1170. [[CrossRef](#)]
62. Tsukaya, H. Leaf shape: Genetic controls and environmental factors. *Int. J. Dev. Biol.* **2005**, *49*, 547–555. [[CrossRef](#)] [[PubMed](#)]
63. Matsuda, S.; Takano, S.; Sato, M.; Furukawa, K.; Nagasawa, H.; Yoshikawa, S.; Kasuga, J.; Tokuji, Y.; Yazaki, K.; Nakazono, M.; et al. Rice Stomatal Closure Requires Guard Cell Plasma Membrane ATP-Binding Cassette Transporter RCN1/OsABCG5. *Mol. Plant* **2016**, *9*, 417–427. [[CrossRef](#)] [[PubMed](#)]
64. Moura, J.C.; Bonine, C.A.; de Oliveira Fernandes Viana, J.; Dornelas, M.C.; Mazzafera, P. Abiotic and Biotic Stresses and Changes in the Lignin Content and Composition in Plants. *J. Integr. Plant Biol.* **2010**, *52*, 360–376. [[CrossRef](#)] [[PubMed](#)]
65. Pereira, L.; Domingues-Junior, A.P.; Jansen, S.; Choat, B.; Mazzafera, P. Is embolism resistance in plant xylem associated with quantity and characteristics of lignin? *Trees* **2018**, *32*, 349–358. [[CrossRef](#)]
66. Bang, S.W.; Lee, D.K.; Jung, H.; Chung, P.J.; Kim, Y.S.; Choi, Y.D.; Suh, J.W.; Kim, J.K. Overexpression of OsTF1L, a rice HD-Zip transcription factor, promotes lignin biosynthesis and stomatal closure that improves drought tolerance. *Plant Biotechnol. J.* **2019**, *17*, 118–131. [[CrossRef](#)]
67. Xu, W.; Tang, W.; Wang, C.; Ge, L.; Sun, J.; Qi, X.; He, Z.; Zhou, Y.; Chen, J.; Xu, Z.; et al. SiMYB56 Confers Drought Stress Tolerance in Transgenic Rice by Regulating Lignin Biosynthesis and ABA Signaling Pathway. *Front. Plant Sci.* **2020**, *11*, 785. [[CrossRef](#)]

68. Sun, S.C.; Xiong, X.P.; Zhang, X.L.; Feng, H.J.; Zhu, Q.H.; Sun, J.; Li, Y.J. Characterization of the Gh4CL gene family reveals a role of Gh4CL7 in drought tolerance. *BMC Plant Biol.* **2020**, *20*, 125. [[CrossRef](#)]
69. Liu, W.; Jiang, Y.; Wang, C.; Zhao, L.; Jin, Y.; Xing, Q.; Li, M.; Lv, T.; Qi, H. Lignin synthesized by CmCAD2 and CmCAD3 in oriental melon (*Cucumis melo* L.) seedlings contributes to drought tolerance. *Plant Mol. Biol.* **2020**, *103*, 689–704. [[CrossRef](#)]
70. Zhao, D.; Luan, Y.; Shi, W.; Zhang, X.; Meng, J.; Tao, J. A *Paeonia ostii* caffeoyl-CoA O-methyltransferase confers drought stress tolerance by promoting lignin synthesis and ROS scavenging. *Plant Sci.* **2021**, *303*, 110765. [[CrossRef](#)]